Optimized supervisory control of a combined heat and power plant by mixed-integer nonlinear model predictive control

Dimitri Bitner[1,*], Artyom Burda[1] and Martin Grotjahn[1]
[1]Hannover University of Applied Sciences and Arts, Hannover, Germany
[*]dimitri.bitner@hs-hannover.de

Abstract

The increasing variety of combinations of different building technology components offers a high potential for energy and cost savings in today's buildings. However, in most cases, this potential is not yet fully exploited due to the lack of intelligent supervisory control systems that are required to manage the complexity of the resulting overall systems. In this article, we present the implementation of a mixed-integer nonlinear model predictive control approach as a smart real-time building energy management system. The presented methodology is based on a forward-looking optimization of the overall energy costs. It takes into account energy demand forecasts and varying electricity market prices. We achieve real-time capability of the controller by applying a decomposition approach, which approximates the optimal solution of the underlying mixed-integer optimal control problem by convexification and rounding of the relaxed solution. The quality of the suboptimal solution is evaluated by comparison with the globally optimal solution obtained by the dynamic programming method. Based on a real-world scenario, we demonstrate that utilization of the real-time capable mixed-integer nonlinear model predictive control approach in a building control system leads to savings of 16% in the total operating costs and 13% in primary energy compared to the state-of-the-art control strategy without any loss of comfort for the residents.

Keywords— *energy management, NMPC, mixed-integer programming, dynamic programming, combined heat and power*

1 Introduction

Structural changes in energy supply and distribution, such as the increase in decentralized generation and storage, the roll-out of smart building and communication technologies, along with the dynamization of the energy markets, lead to an increase in complexity in today's energy supply systems. The complexity is also particularly evident at the building level. In today's buildings, there is a wide variety of combinations of different components such as boilers, combined heat and power units, solar/photovoltaic systems, thermal/electric storage units, ventilation systems, etc. All actions in this area follow the joint goal of increasing living comfort, while at the same time maximizing energy efficiency and minimizing energy costs. However, these competing goals, in addition to the complexity, are also one of the main reasons why there is still great potential for optimization of the energy management of buildings in practice. According to [1, 2], energy savings of up to 30% can be achieved through improved connectivity and intelligent operation management of building components. Model predictive control (MPC) is getting more widespread and can be considered as a promising tool to exploit these potentials [3]. The (nonlinear) MPC is suitable for the control of (nonlinear) multivariable systems and has the decisive ability to predictively take into account constraints on the control and state variables of the system. These features make the MPC ideally suited as predictive supervisory control of buildings' energy management. This has already been demonstrated in various studies, such as [4, 5, 6].

Within this paper, we present the setup of mixed-integer nonlinear model predictive control (MI-NMPC) for supervisory control of a residential combined heat and power plant for the first time. Due to the discrete on/off characteristics in addition to the continuously modulable operating range of the components used in such energy supply systems, the corresponding optimization problem results in a mixed-integer optimal control problem (MIOCP). For solving these particular problems, methods such as dynamic programming [7, 8] or branch-and-bound algorithms [9, 10, 11] exist, as well as corresponding solvers such as the open-source solver Bonmin [10]. However, these methods attempt to determine the exact solution. Therefore, they are often only suitable for applications with small prediction horizons, since problem complexity and, thus, the computation time for solving increase exponentially with the horizon [4]. As a remedy, we use the decomposition approach, first introduced in [12], to determine an approximated solution for the original MIOCP in significantly reduced time. This approach has already been successfully applied to e.g. the fuel energy management for a hybrid electric vehicle [13] and the optimization of chromatographic processes [14].
For the aforementioned practical application, we determine the energy and cost saving potential (global optimal solution) by solving the MIOCP with dynamic programming offline (open-loop control) and compare the results with the state-of-the-art control strategy. In this context, we also investigate the impact of varying electricity market prices on the total costs within the optimal control system. Subsequently, we evaluate the

ISBN 978-3-8007-5651-3

quality of the suboptimal solution obtained by the new real-time capable approach in a closed-loop simulation.
The article is structured as follows. First, we describe the considered power supply system and the resulting optimization task. Next, a presentation of the modeling approach follows. In Section 3 the general formulation of the MIOCP is introduced and the previously mentioned control methodology together with the reformulations of the MIOCP, required for implementation, are presented. Based on numerical results, we show the achievable savings as well as the real-time capability of the presented approach and close the article with conclusions and an outlook on future work.

2 Building Energy Supply System

2.1 System Description and Problem Definition

The energy supply system considered here is a combination of components, typically found in residential buildings supplied by combined heat and power (CHP) units. As shown in **Figure 1**, the system consists of a gas-driven modulating micro-CHP unit, a condensing boiler, which can be used as a backup heater, and a buffer storage tank. Generated thermal energy is stored in the buffer tank and, when required, is used for heating and as a source of domestic hot water. The electricity, generated by the CHP unit, is used on demand in the house. The excess energy is fed into the public power grid - conversely, a lack of electrical energy is covered from the grid. Hence, the system has different energy sources, each with different efficiencies and costs. Moreover, the CHP unit generates electricity and heat simultaneously, but both types of energy are not always needed at the same time and the storage tank has only limited capacity for buffering. The operation of CHP units in single- and multi-family houses is typically limited only to the control of thermal energy - similar to classical heating control. This is done in order to ensure the thermal demand and, thus, to fulfill the most important user requirement. The electrical energy is generated independently of the user's demands. Therefore, a large part of the generated energy is fed into the grid which results in considerable financial losses. This can directly be seen by the energy prices, which in our case are $c_1 = 5.31$ cents/kWh for the gas purchase and an average value of $c_3 = 26.06$ cents/kWh for the electricity purchase from the grid. Furthermore, the customer receives payments of $c_4 = 4$ cents for each self-generated kWh (regardless of feed-in or own use) and $c_2 = 8.67$ cents/kWh for the feed-in of self-generated electrical energy. With a maximum electrical efficiency of about 25%, it is directly clear that the feed-in itself cannot be an economic goal. In fact, the greatest cost savings occur in the opposite case, namely, in avoiding the comparatively high electricity purchase costs, i.e. in maximizing the use of in-house electricity. At the same time, however, the simultaneous thermal energy generation vs. current and future thermal demand/buffer storage capacity and occupant comfort requirements must always be taken into account. This leads to a multiobjective economic optimal control problem (OCP).

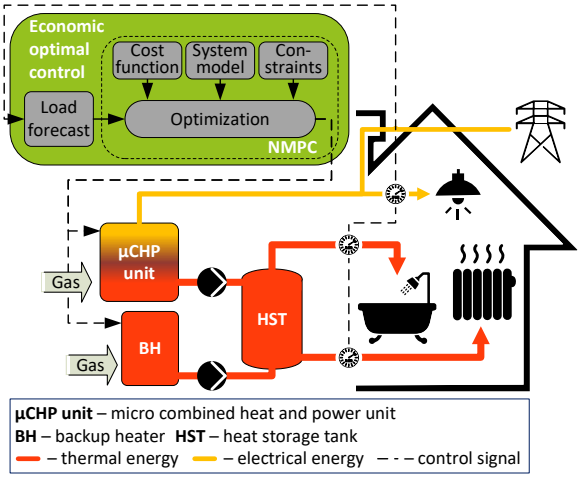

Figure 1 Scheme of control approach and energy system

We propose an approach to solve the resulting problem by use of advanced control engineering methods, i.e. by combining an energy demand prediction, which is based on machine learning methods, with a MI-NMPC strategy. The optimal operating strategy of the overall system is calculated with consideration of the total operating costs, constraints and energy demands for the next 24 hours.

2.2 Modeling Approach

The nonlinear model of the energy supply system, used for simulation and control, represents the energy exchange between the individual components and the surroundings. Thus, it is based on the electrical and thermal efficiency curves of the generators and takes into account losses to the environment. The class of variables is composed of the electrical power P, the thermal power $\dot{Q}$, u_i as general input power and the binary input variable v_i describing the on/off state of the devices. All parameters of the model are summarized in **Table 1**. The input and control variable of the CHP unit is the electrical generation power

$$P_{\mathrm{chp}}(t) = u_1(t)v_1(t), \tag{1}$$

which can be modulated continuously in the range of $u_1 =$ 1.65 - 4.55 kW when switched on ($v_1 = 1$) and is zero when switched off ($v_1 = 0$). The heating power of the gas $\dot{Q}_{\mathrm{g,chp}}$, which is consumed during operation, based on the higher heating value, is calculated from the electrical efficiency characteristic η_{e} of the CHP unit

$$\dot{Q}_{\mathrm{g,chp}}(t) = \frac{P_{\mathrm{chp}}(t)}{\eta_{\mathrm{e}}(P_{\mathrm{chp}}(t))} = \frac{P_{\mathrm{chp}}(t)}{a_0 + a_1 P_{\mathrm{chp}}^2(t) + a_2 P_{\mathrm{chp}}(t)}. \tag{2}$$

For the electrical efficiency curve, a quadratic relationship is assumed according to [15] (see **Figure 2**). Moreover, Eq. (2) already takes into account the electric self-consumption of the CHP unit during operation. The thermal power $\dot{Q}_{\mathrm{chp}}$ is derived from Eq. (2), extended by the thermal efficiency curve η_{q}. The thermal efficiency is

Table 1 Parameters of the energy system model

Name	Description	Unit	Value
a_0	Coefficient of steady-	-	0.2
a_1	state electr. conversion	W^{-2}	-4.2e-9
a_2	efficiency of CHP unit	W^{-1}	4.0e-5
b_0	Coefficient of steady-	-	0.1
b_1	state thermal efficiency	W^{-2}	-4.3e-8
b_2	of CHP unit	W^{-1}	3.0e-4
A	Surface of storage	m^2	5.5
c_w	Specific heat capacity	Ws/(kgK)	4190
d_0	Coefficient of electr.	W	15.7
d_1	consumption of boiler	-	2.0e-3
d_2	Coefficient of thermal	W^{-1}	-1.5e-6
d_3	efficiency of boiler	-	9.9e-1
H_{fil}	Heat loss coefficient	W/K	3
H_{sto}	Heat loss coefficient	$W/(m^2K)$	0.5
m	Storage water mass	kg	900
ΔT_{chp}	temperature difference	K	80
ΔT_{boi}	temperature difference	K	65

also modeled by a quadratic characteristic (see **Figure 2**). We take into account the thermal losses of the CHP unit during operation and energy transfer to the buffer storage tank by subtracting a constant factor. This factor equals the multiplication of the heat loss coefficient H_{fil} and the sum of the average temperature differences ΔT_{chp} between the individual components and the surroundings. The resulting equation reads

$$\begin{aligned}\dot{Q}_{chp}(t) &= \frac{P_{chp}(t)\eta_q(P_{chp}(t))}{\eta_e(P_{chp}(t))} - H_{fil}\Delta T_{chp} v_1(t) \\ &= \frac{P_{chp}(t)(b_0 + b_1 P_{chp}^2(t) + b_2 P_{chp}(t))}{a_0 + a_1 P_{chp}^2(t) + a_2 P_{chp}(t)} \\ &\quad - H_{fil}\Delta T_{chp} v_1(t).\end{aligned} \tag{3}$$

The input and control variable of the condensing boiler is the heating power of the gas

$$\dot{Q}_{g,boi}(t) = u_2(t) v_2(t), \tag{4}$$

which, analogous to the CHP unit, can be modulated continuously in the range of u_2 = 6 - 32 kW when switched on (v_2 = 1) or is zero in the other case (v_2 = 0). The thermal output power $\dot{Q}_{boi}$ is derived from a linear efficiency characteristic from 94% to 98% related to the higher heating value

$$\dot{Q}_{boi}(t) = d_2 \dot{Q}_{g,boi}^2(t) + d_3 \dot{Q}_{g,boi}(t) - H_{fil}\Delta T_{boi} v_2(t). \tag{5}$$

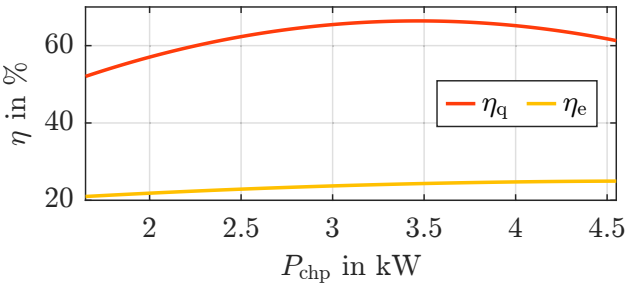

Figure 2 Thermal and electrical efficiency of CHP unit

Thermal losses to the environment during the generation and distribution processes are also taken into account analogously to the CHP unit. For the sum of the temperature differences, the corresponding parameter ΔT_{boi} is used due to the lower supply temperature of the boiler. In addition to the gas, the condensing boiler also consumes a small amount of electrical power P_{boi} during operation. This is taken into account by the linear relationship

$$P_{boi}(t) = d_1 \dot{Q}_{g,boi}(t) + d_0 v_2(t). \tag{6}$$

The models of the power generation facilities consider only the steady-state energy conversion processes. The time constants of the dynamic processes, due to the heating up and cooling down phases of the components, are below the sampling times of the controller, considered here. E.g. even after the facilities are switched off, the residual heat is almost completely transported to the storage tank in a comparatively short time. In addition, when considering only the energy exchange, the heating up and cooling down effects mainly balance each other out and are therefore neglected. The buffer storage tank is modeled by use of the incoming and outgoing thermal powers. The input variables are the thermal powers of the power generation facilities and the demand from the building $\dot{Q}_{con}$. The sum of these powers minus the ambient losses, integrated over time, results in the thermal energy of the storage tank Q_{sto}. Here, the losses are calculated by the heat loss coefficient H_{sto} and the surface A of the storage tank, the water mass m, the specific heat capacity c_w and Q_{sto}. Thus, the thermal energy in the storage tank is modeled by the following first-order differential equation

$$\begin{aligned}\dot{Q}_{sto}(t) &= \dot{Q}_{chp}(t) + \dot{Q}_{boi}(t) - \dot{Q}_{con}(t) \\ &\quad - H_{sto}\frac{A}{m c_w} Q_{sto}(t).\end{aligned} \tag{7}$$

Since the storage model does not represent temperatures and volume flows, effects such as convection and conduction are not considered.

The last model component consists of the energy sinks within the overall system, which in our case are composed of the thermal and electrical consumptions $\dot{Q}_{con}$ and P_{con} in the building. The electrical consumption is needed to calculate the total energy costs. From a control point of view, the consumption data corresponds to input variables that cannot be manipulated and are provided by measurements or, when the model is used within a predictive controller, results from an external energy demand forecast.

3 Mixed-Integer Optimal Control

In this section, we first introduce the considered optimization problem. The problem statement is then reformulated by appropriate algorithms to guarantee real-time applicability.

ISBN 978-3-8007-5651-3

3.1 Problem Formulation

The goals of operating an energy supply system are minimizing the overall energy costs while at the same time ensuring permanent supply of the required energy. As mentioned in Section 2, this results in a multiobjective economic optimal control problem that evaluates the total operating costs in the objective function. More specifically, the total costs consist of the costs for the gas consumption of the producers (weighted by the gas price c_1), the remuneration for self-generated electricity (weighted by c_4) and the costs for electricity purchases from the grid (weighted by c_3) or payments for feeding into the grid (weighted by c_2). This results in the Lagrange term

$$\begin{aligned} l(t,\boldsymbol{u}(t),\boldsymbol{v}(t),P_{\text{con}}(t)) = \\ &(\dot{Q}_{\text{g,chp}}(t)+\dot{Q}_{\text{g,boi}}(t))c_1 - P_{\text{chp}}(t)c_4 \\ &+(1-v_3(t))(P_{\text{con}}(t)+P_{\text{boi}}(t)-P_{\text{chp}}(t))c_3 \\ &+v_3(t)(P_{\text{con}}(t)+P_{\text{boi}}(t)-P_{\text{chp}}(t))c_2. \end{aligned} \tag{8}$$

The electricity price changes depending on whether electrical energy is fed into or drawn from the grid. This distinction is taken into account by an additional binary control function v_3. To ensure the correct assignment, the following must hold

$$v_3(t) = \begin{cases} 1 \text{ for } P_{\text{con}}(t)+P_{\text{boi}}(t) \le P_{\text{chp}}(t) \\ 0 \text{ for } P_{\text{con}}(t)+P_{\text{boi}}(t) > P_{\text{chp}}(t) \end{cases}, \tag{9}$$

which is realized by means of the nonlinear constraints

$$(1-v_3(t))(P_{\text{chp}}(t)-P_{\text{con}}(t)-P_{\text{boi}}(t)) \le 0, \tag{10}$$

$$v_3(t)(P_{\text{con}}(t)+P_{\text{boi}}(t)-P_{\text{chp}}(t)) \le 0. \tag{11}$$

The resulting MIOCP reads

$$\begin{aligned} \min_{\boldsymbol{u}(\cdot)\boldsymbol{v}(\cdot)} \quad & \int_{t_0}^{t_\text{f}} l(\boldsymbol{u}(t),\boldsymbol{v}(t),P_{\text{con}}(t))\mathrm{d}t \\ \text{s.t.} \quad & \dot{Q}_{\text{sto}}(t) = f(Q_{\text{sto}}(t),\boldsymbol{u}(t),\boldsymbol{v}(t),\dot{Q}_{\text{con}}(t)), \\ & Q_{\text{sto}}(t_0) = Q_0, \\ & Q_{\text{sto}}(t) = [Q_{\min},Q_{\max}] && \text{for } t\in[t_0,t_\text{f}], \\ & \boldsymbol{u}(t) = [\boldsymbol{u}_{\min},\boldsymbol{u}_{\max}] && \text{for } t\in[t_0,t_\text{f}], \\ & \boldsymbol{0} \ge \boldsymbol{c}(\boldsymbol{u}(t),\boldsymbol{v}(t),P_{\text{con}}(t)) && \text{for } t\in[t_0,t_\text{f}], \\ & \boldsymbol{v}(t) \in \{0,1\}^3 && \text{for } t\in[t_0,t_\text{f}], \end{aligned} \tag{12}$$

where Q_{sto} represents the system state corresponding to the thermal energy stored in the tank, $\boldsymbol{u}^\text{T} = [u_1,u_2]$ the vector of continuous control variables, $\boldsymbol{v}^\text{T} = [v_1,v_2,v_3]$ the vector of binary control variables and $\boldsymbol{c}^\text{T}$ the vector of the constraints in Eq. (10) and (11). For the state Q_{sto} and the controls, additional point and path constraints (i.e. boundary values) apply.

3.2 Convexification and Relaxation

Within a MI-NMPC, the MIOCP (12) is solved for a finite time horizon, here $T = 24$ h, in each time step. However, only the first values of the calculated optimal control variable sequences are used for the process control. At the next time step, the optimization is repeated for the new shifted time horizon with the updated states. Thus, the optimal open-loop control is transferred into closed-loop control. Consequently, the available duration of solving the MIOCP is limited by the sample time, which in our case is $T_\text{S} = 10$ min. Therefore, in the context of MI-NMPC, we determine an approximated solution for the MIOCP (12) based on the ideas in [12] by executing the following steps:

1) Reformulate the MIOCP (12) by means of outer convexification.
2) Solve a continuous relaxation of the reformulated problem.
3) Compute the Sum-Up Rounding strategy (SUR) from [12] on the relaxed optimal solution to obtain an integer feasible control trajectory for the discrete control variables.

We apply the outer convexification by introducing a new binary control function ω_i for each possible choice of $\boldsymbol{v}(t) = \boldsymbol{w}_i \in \{(0,0,0),(0,0,1),\ldots,(1,1,1)\}$. The equivalent reformulation of (12) reads

$$\begin{aligned} \min_{\boldsymbol{u}(\cdot)\boldsymbol{\omega}(\cdot)} \quad & \sum_{i=1}^{8} \int_{t_0}^{t_\text{f}} l(\boldsymbol{u}(t),\boldsymbol{w}_i,P_{\text{con}}(t))\omega_i(t)\mathrm{d}t \\ \text{s.t.} \quad & \dot{Q}_{\text{sto}}(t) = \sum_{i=1}^{8} f(Q_{\text{sto}}(t),\boldsymbol{u}(t),\boldsymbol{w}_i,\dot{Q}_{\text{con}}(t))\omega_i(t), \\ & Q_{\text{sto}}(t_0) = Q_0, \\ & Q_{\text{sto}}(t) = [Q_{\min},Q_{\max}] && \text{for } t\in[t_0,t_\text{f}], \\ & \boldsymbol{u}(t) = [\boldsymbol{u}_{\min},\boldsymbol{u}_{\max}] && \text{for } t\in[t_0,t_\text{f}], \\ & \boldsymbol{0} \ge \boldsymbol{c}(\boldsymbol{u}(t),\boldsymbol{w}_i,P_{\text{con}}(t))\omega_i(t) && \text{for } t\in[t_0,t_\text{f}], \\ & \boldsymbol{\omega}(t) \in \{0,1\}^8 && \text{for } t\in[t_0,t_\text{f}], \\ & 1 = \sum_{i=1}^{8} \omega_i(t) && \text{for } t\in[t_0,t_\text{f}]. \end{aligned} \tag{13}$$

In our particular case, two of the newly introduced binary control functions and 12 of the $2\cdot 8 = 16$ constraints can be omitted, since in practice those constraints are either always satisfied regardless of ω_i or can never be satisfied for $\omega_i = 1$. Thus, the optimizer would never activate those cases, which is why a definition of these control functions and associated constraints is superfluous.

Relaxation of the binary control functions $\boldsymbol{\omega}$ results in the nonlinear continuous OCP

$$\begin{aligned} \min_{\boldsymbol{u}(\cdot)\boldsymbol{\alpha}(\cdot)} \quad & \sum_{i=1}^{6} \int_{t_0}^{t_\text{f}} l(\boldsymbol{u}(t),\boldsymbol{w}_i,P_{\text{con}}(t))\alpha_i(t)\mathrm{d}t \\ \text{s.t.} \quad & \dot{Q}_{\text{sto}}(t) = \sum_{i=1}^{6} f(Q_{\text{sto}}(t),\boldsymbol{u}(t),\boldsymbol{w}_i,\dot{Q}_{\text{con}}(t))\alpha_i(t), \\ & Q_{\text{sto}}(t_0) = Q_0, \\ & Q_{\text{sto}}(t) = [Q_{\min},Q_{\max}] && \text{for } t\in[t_0,t_\text{f}], \\ & \boldsymbol{u}(t) = [\boldsymbol{u}_{\min},\boldsymbol{u}_{\max}] && \text{for } t\in[t_0,t_\text{f}], \\ & \boldsymbol{0} \ge \boldsymbol{c}(\boldsymbol{u}(t),\boldsymbol{w}_i,P_{\text{con}}(t))\alpha_i(t) && \text{for } t\in[t_0,t_\text{f}], \\ & \boldsymbol{\alpha}(t) \in [0,1]^6 && \text{for } t\in[t_0,t_\text{f}], \\ & 1 = \sum_{i=1}^{6} \alpha_i(t) && \text{for } t\in[t_0,t_\text{f}]. \end{aligned} \tag{14}$$

ISBN 978-3-8007-5651-3

Note: The considered system has another constraint, which is not yet considered in the above formulations. To reduce the wear of the CHP unit due to frequent startup and shutdown, the device has a minimum operation time of 60 min after each activation. Such minimum dwell times cannot be represented in the solution of a continuous OCP and, therefore, have to be considered in the rounding in step 3. The consideration of dwell times in the solution of MIOCPs is part of future work.

4 Numerical Results

Within this section, we show numerical results obtained by the cost-optimal operation of the considered energy supply system. We first determine the achievable energy and cost saving potential by comparing an offline (open-loop) optimal control with the classical operation strategy. Then, the real-time computation of the approximated solution is performed online (closed-loop) and the achievable optimality is investigated. The simulation sample time is T_S = 10 min. We use real consumption data, measured with high temporal resolution (1-second cycle), for both simulation and prediction of the energy consumption ("exact prediction").

4.1 Dynamic Programming vs. State-of-the-Art Control Strategy

To determine the globally optimal solution dynamic programming is used. In this method, problem (12) is solved recursively by dividing it into subproblems and storing the intermediate results [7]. This technique is constrained by the "curse of dimensionality" and is, therefore, used as an online optimization strategy only for small-size problems. For the optimization problem considered here, the computation time of dynamic programming, needed to solve the problem, significantly exceeds the sample time. However, it is ideally suited for offline investigation of the potential of an optimization approach compared to a classical strategy. In the setup of the optimal control, we additionally consider two different approaches: taking 1) constant and 2) varying electricity market prices into account within the optimal control system. The OCPs are solved by means of the *dpm*-function from [16] in Matlab.

In **Figure 3** one can see the trajectories for the different control methods together with the main influencing variables. These are the outside temperature, the electricity prices on the European Energy Exchange (EEX) and the electrical and thermal energy consumption. To achieve the goal of minimizing the total operating costs, the dynamic programming optimizer (DP) exploits the information about the future energy demands and shifts the operating hours of the CHP unit to the electrical peak load periods whenever possible (see electrical power consumption and generated power in the center plot in **Figure 3**). The capacity of the buffer storage is fully utilized to bridge periods of low electrical consumption (see bottom plot in **Figure 3**). As a result, the amount of in-house electricity is maximized while uneconomical feed-in is minimized. At the same time, thermal energy needs are consistently met (no overrun of the 13.5 and 50 kWh storage limits occur). In contrast, the heat-led control strategy (SoA) is mainly based on the level of the storage tank and the outdoor temperature. Predefined day times for low, medium or high production are used to specify the desired level of the storage tank. This way, a higher overall level is maintained

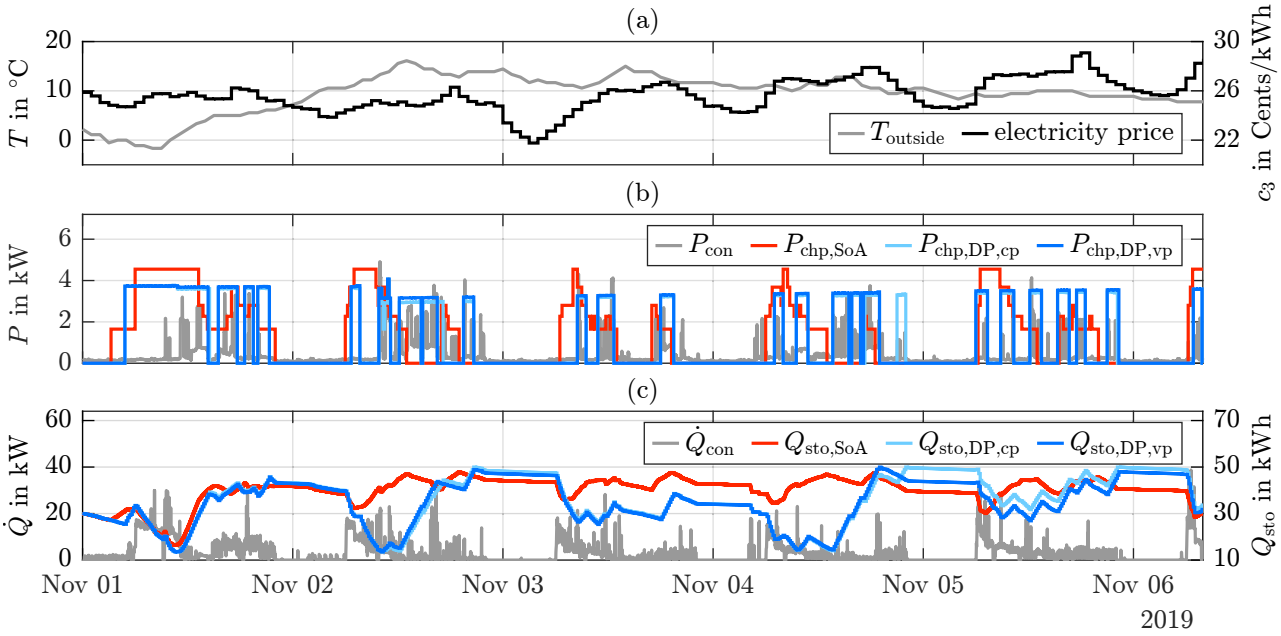

Figure 3 Characteristics of the power supply system - (a) outside temperature $T_{outside}$ and price of electricity c_3, (b) electrical power consumption P_{con} and generated power P_{chp} and (c) thermal power consumption $\dot{Q}_{con}$ and energy Q_{sto} in storage with heat-led control strategy (SoA) and dynamic programming approach (DP) with constant (cp) and varying (vp) electricity price

in the storage tank. The future demand is not known in advance and the controller, therefore, always tries to keep sufficient thermal energy for high consumption times, e.g. on the first day of the simulation.
The boiler serves as a backup heater and is only used when there is a high thermal demand on very cold days. In the period under consideration, support by the backup heater is not required at any time.
Table 2 summarizes the savings of the optimal control approach with constant (cp) and varying (vp) electricity prices compared to the state-of-the-art control strategy for a period of 7 days. Here, one can also see that the additional consideration of varying electricity prices brings further cost savings. However, these extra savings are comparatively low due to the small price fluctuation. From a financial point of view, often it is not reasonable to shift the electricity production of the CHP unit from the peak load to the lower price periods.

Table 2 Savings of dynamic programming (DP) compared to SoA-control strategy for a period of 7 days

	Operat. costs	Gas consum.	Elect. feed	Elect. purchase
DP,cp	-16.5%	-12.8%	-16.5%	-32.3%
DP,vp	-16.6%	-13.1%	-16.0%	-30.0%

4.2 Mixed-integer Real-Time Solution

The methodology described in Section 3.2 is used to determine an approximated solution of the optimization problem (12) in real-time. The calculations are carried out using the Matlab interface of the numerical optimal control software package *acados* [17]. In *acados*, a multiple shooting approach is used to discretize the OCP. We solve the resulting Nonlinear Program (NLP) by means of the implemented *SQP_RTI* technique [18] using the interior-point method solver *HPIPM* for quadratic programs [19] in a MI-NMPC strategy. E.g. an approximated solution of the problem (14) is determined at each time step and, after rounding, the control variables are fed back to the process (closed-loop simulation). For the boundaries on the state variable and Eq. (10) and (11) we use soft constraints, i.e. violation of the limits is allowed within the optimization, but will be punished with penalty costs.
We compare the MI-NMPC solution with the globally optimal solution obtained by dynamic programming to evaluate the quality of the real-time capable suboptimal solution. Both approaches consider varying electricity prices. The deviations of the savings in operational costs, gas consumption and electrical feed and purchase are shown in **Table 3**.

Table 3 Deviation of MI-NMPC solution from globally optimal solution for a period of 7 days

Operational costs	Gas consumpt.	Electrical feed	Electrical purchase
0.3%	0.2%	0.7%	2.3%

Figure 4 illustrates the resulting trajectories of the generated electrical power and thermal energy level in the storage together with the electrical and thermal consumption. The trajectories of the approximated solution partly show slight deviations from the globally optimal curves, both in the power value and the on/off periods. In total, the MI-NMPC still achieves high agreement with the globally optimal solution. This becomes particularly evident considering the cost differences in **Table 3**, which deviate by only 0.3% for a period of 7 days. However, with a computation time of less than one second, the presented real-time capable approach is faster by a factor of 1000, compared to dynamic programming.

5 Conclusions

We presented a new approach for the supervisory control of building energy supply systems that enables significant energy and cost savings without the need for additional technical modifications. Our control strategy performs an

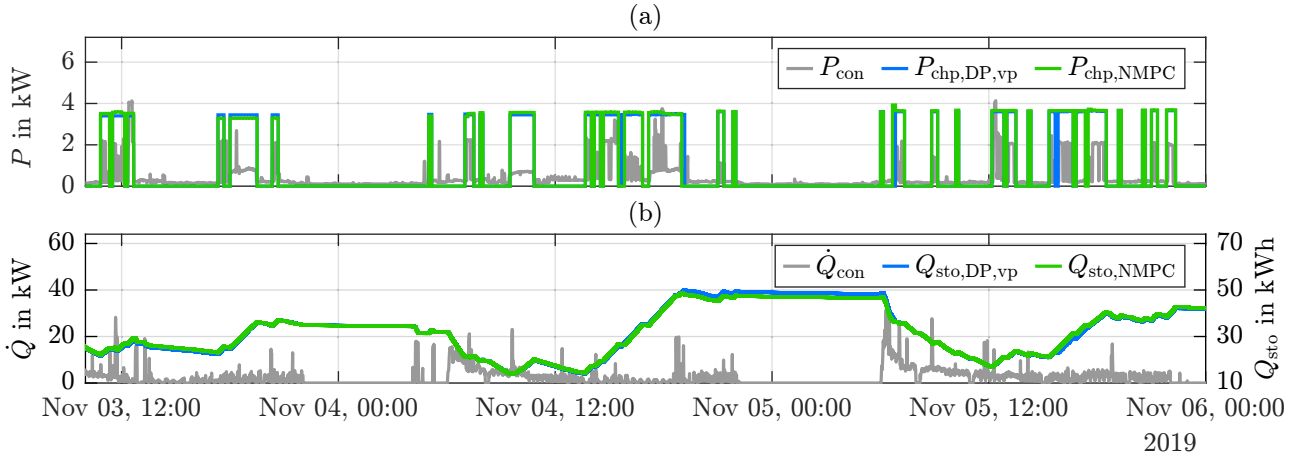

Figure 4 Characteristics of the power supply system - (a) electrical power consumption P_{con} and generated power P_{chp} and (b) thermal power consumption $\dot{Q}_{con}$ and energy Q_{sto} in storage with dynamic programming (DP,vp) and MI-NMPC (NMPC) approach

online optimization of the operating modes based on a model of the system to be controlled. It was applied to an energy supply system, where savings of up to 16.6% in the total operating costs and 13.1% in primary energy were achieved. The present optimization routine results in a mixed-integer optimal control problem (MIOCP), whose exact solution requires a high computational effort. By reformulating the MIOCP using direct convexification and relaxation, a continuous OCP results. This leads to a significant reduction of computational time. Subsequent rounding of the discrete control variables yields an approximated discrete solution. We have shown in a closed-loop simulation that the results obtained by a MI-NMPC strategy based on the presented approach achieve high agreement with the globally optimal solution. As consequence, the cost and energy saving potential is almost completely exploited while the practice-relevant property of real-time capability is fulfilled by our control technique. Future work will investigate the consideration of dwell-times within the optimization algorithm as well as the influence of load prediction deviations on the achievable optimality. In addition, the presented control strategy will be implemented in practice in a real building.

6 Literature

[1] A. Costa, M. M. Keane, J. I. Torrens, and E. Corry, "Building operation and energy performance: Monitoring, analysis and optimisation toolkit," Applied Energy, vol. 101, pp. 310–316, 2013, doi: 10.1016/j.apenergy.2011.10.037.

[2] D. Zhou and S. H. Park, "Simulation-Assisted Management and Control Over Building Energy Efficiency – A Case Study," Energy Procedia, vol. 14, pp. 592–600, 2012, doi: 10.1016/j.egypro.2011.12.980.

[3] P. H. Shaikh, N. B. M. Nor, P. Nallagownden, I. Elamvazuthi, and T. Ibrahim, "A review on optimized control systems for building energy and comfort management of smart sustainable buildings," Renewable and Sustainable Energy Reviews, vol. 34, pp. 409–429, 2014, doi: 10.1016/j.rser.2014.03.027.

[4] A. Bürger, C. Zeile, A. Altmann-Dieses, S. Sager, and M. Diehl, "An Algorithm for Mixed-Integer Optimal Control of Solar Thermal Climate Systems with MPC-Capable Runtime," in 2018 European Control Conference (ECC), 2018, pp. 1379–1385.

[5] G. Bruni, S. Cordiner, V. Mulone, V. Sinisi, and F. Spagnolo, "Energy management in a domestic microgrid by means of model predictive controllers," Energy, vol. 108, pp. 119–131, 2016, doi: 10.1016/j.energy.2015.08.004.

[6] W. Bosschaerts, T. van Renterghem, O. A. Hasan, and K. Limam, "Development of a Model Based Predictive Control System for Heating Buildings," Energy Procedia, vol. 112, pp. 519–528, 2017, doi: 10.1016/j.egypro.2017.03.1110.

[7] D. P. Bertsekas, Dynamic programming and optimal control, 3rd ed. Belmont, Mass.: Athena Scientific, 2005.

[8] E. Hellström, M. Ivarsson, J. Åslund, and L. Nielsen, "Look-ahead control for heavy trucks to minimize trip time and fuel consumption," Control Engineering Practice, vol. 17, no. 2, pp. 245–254, 2009, doi: 10.1016/j.conengprac.2008.07.005.

[9] I. Quesada and I. E. Grossmann, "An LP/NLP based branch and bound algorithm for convex MINLP optimization problems," Computers & Chemical Engineering, vol. 16, 10-11, pp. 937–947, 1992, doi: 10.1016/0098-1354(92)80028-8.

[10] P. Bonami et al., "An algorithmic framework for convex mixed integer nonlinear programs," Discrete Optimization, vol. 5, no. 2, pp. 186–204, 2008, doi: 10.1016/j.disopt.2006.10.011.

[11] M. Gerdts, "Solving mixed-integer optimal control problems by branch&bound: a case study from automobile test-driving with gear shift," Optim. Control Appl. Meth., vol. 26, no. 1, pp. 1–18, 2005, doi: 10.1002/oca.751.

[12] S. Sager, Numerical methods for mixed-integer optimal control problems. Zugl.: Heidelberg, Univ., Diss., 2005. Tönning: Der Andere Verl., 2005.

[13] N. Robuschi, C. Zeile, S. Sager, and F. Braghin, "Multiphase mixed-integer nonlinear optimal control of hybrid electric vehicles," Automatica, vol. 123, p. 109325, 2021, doi: 10.1016/j.automatica.2020.109325.

[14] H. Bock, Dominik H. Cebulla, C. Kirches, Andreas, and Potschka, "Mixed-Integer Optimal Control for Multimodal Chromatography," 2020. [Online]. Available: https://www.semanticscholar.org/paper/Mixed-Integer-Optimal-Control-for-Multimodal-Bock-Cebulla/d708d86d1141c3c2205f613490b38fc905c9ffc0

[15] I. Beausoleil-Morrison and N. Kelly, "Specifications for modelling fuel cell and combustion-based residential cogeneration device within whole-building simulation programs," 2007.

[16] O. Sundstrom and L. Guzzella, "A generic dynamic programming Matlab function," in 2009 IEEE Control Applications, (CCA) & Intelligent Control, (ISIC), 2009, pp. 1625–1630.

[17] R. Verschueren et al., "acados: a modular open-source framework for fast embedded optimal control," 2019. [Online]. Available: https://arxiv.org/pdf/1910.13753

[18] R. Verschueren, "Convex approximation methods for nonlinear model predictive control," 2018.

[19] G. Frison and M. Diehl, "HPIPM: a high-performance quadratic programming framework for model predictive control," 2020. [Online]. Available: https://arxiv.org/pdf/2003.02547